



Effect of acidic environment on absorptive, morphological, mechanical, structural, and thermal properties of glass-carbon/epoxy-based hybrid composites

Tarkan Akderya¹ · Nesrin Horzum² · Buket Okutan Baba³

Received: 24 October 2023 / Accepted: 22 December 2023
© The Polymer Society, Taipei 2024

Abstract

This study experimentally investigated the effects of acidic environments on the absorptive, morphological, mechanical, structural, and thermal properties of glass-carbon/epoxy-based hybrid composites. For this purpose, hybrid composite specimens were conditioned by immersion in an acidic environment with pH 1.0 at -10, 25, and 40 °C for different periods (1 day, 1–3–6–9–12 weeks). A comparative study was conducted to evaluate the properties of dry and acid-immersed specimens and to examine failures due to the acidic environment and temperature. It has been observed that all properties of hybrid composites are significantly affected by acidic environmental conditions, and failure development is highly dependent on acidic ambient temperature and exposure time.

Keywords Woven glass/carbon fibre · Epoxy · Hybrid · Acidic environment · Ageing · Characterisation

Introduction

Composite materials are used in many applications and fields for their outstanding properties, such as high strength, rigidity, design capability, and lightness. These prominent features have made these materials an alternative to metallic materials [1–3]. Despite these positive developments, research on “hybridisation” has come to the fore due to the vital need for light and inexpensive new materials with improved strength values [4, 5]. Fibre hybridisation is one of several promising strategies used in structural components in different industries to enhance reinforcing material failure strain and reduce cost where the high weight of conventional materials is a significant barrier. In order to collect many

desired properties in a single material and achieve a better balance in properties, hybrid composites with more than one fibre type in the same structure were needed [6].

Hybrid composite materials became one of the research topics in the seventies. Interest and discussion towards the hybrid effect have increased with Hayashi [7] revealing that the fracture strain of carbon fibre layers in the carbon fibre composite material is 40% lower than that of the carbon/glass hybrid composite material. The hybrid effect has been studied by many researchers in order to understand and model the subject. The main principle responsible for the hybrid effect includes residual thermal stresses due to differences in the thermal expansion of different fibres [8, 9]. In addition, the formation of fibre clusters of fibre breaks [10–12] and dynamic stress concentrations [13], which cause changes in damage development, may also be effective in this mechanism. A review article on fibre hybridisation in polymer composites was recently published by Swolfs et al. [6]. Although the hybrid effect is well-defined, it is not yet fully understood. Research to explain the primary mechanism of the hybrid effect is limited and insufficient to observe the complex interaction.

Today, as a result of intensive research and development activities on hybridisation in layered composite materials, hybrid composites are frequently encountered as structural components in the automotive [14, 15], aviation [16, 17],

✉ Tarkan Akderya
tarkan.akderya@bakircay.edu.tr

¹ Department of Biomedical Engineering, Faculty of Engineering and Architecture, University of Bakırçay, Menemen, Izmir, Turkey

² Department of Engineering Sciences, Faculty of Engineering and Architecture, Izmir Katip Çelebi University, Çiğli, Izmir, Turkey

³ Department of Mechanical Engineering, Faculty of Engineering and Architecture, Izmir Katip Çelebi University, Çiğli, Izmir, Turkey

railways [18, 19], marine [20, 21], and wind energy [22, 23] industries. Specifically, automobile structural applications [24], aircraft decks [25], marine applications [26], boat hulls [27, 28], catamaran hull constructions [29], rotor blades of some helicopters [30], ship sonar domes and radomes [31], and wind turbine blades [32, 33] can be given as examples. Due to the diversity in structural applications, these composites may be exposed to environmental effects such as changing temperature, humidity, and liquid or gaseous chemicals during use. Avoiding these environmental factors affecting short- and long-term performance of materials is impossible. Therefore, it is essential to understand how these composite materials behave in ecological conditions with varying properties. However, to obtain the best material properties in different applications, it is necessary to clearly understand the environmental effects on the properties of composite materials during production and use [34].

One of the environments where the ageing effects of hybrid composites can be seen is acidic environments such as acid mine lakes and acid rains. Acid rain occurs due to the reaction of water vapour in the atmosphere, sulfur and nitrogen-containing gases released by coal and fossil fuels into the atmosphere in regions where industrialisation is intense. As a result of these reactions, sulfuric acid and nitric acid droplets fall to the earth through rain, fog, snow, gases, or particles in the air [35]. Acid mine lakes (where the water–rock interaction is intense), another exposure area, occur with the oxidation of iron sulfide minerals in the atmospheric environment, bacteria acting as a catalyst in the background, and some other involved metals in the process. It is formed by acid mine/rock drainage, the accumulation of natural surface and underground waters into the depression formed during or after the open mining operation [36, 37]. It is necessary to be prepared for this effect, which is faced by increasing industrial activities and is more likely to be encountered in the future. Such environments are increasing day by day, and low pH values cause rapid deformation of materials. With innovative materials to be used in these environments, a considerable economic contribution should be provided by minimising engineering problems (notably in mining, maritime sectors and related business lines).

The effects of acidic environments on fibre-reinforced polymer composites have been the subject of numerous studies. The influence of acids on E-glass fibres was investigated by Qiu and Kumosa [38], and they revealed that acid causes axial and spiral cracks on the fibre surface, and, in addition, acid corrosion of E-glass fibres is mainly due to loss of calcium and aluminium ions. They noted that the phenomenon that significantly accelerates fibre corrosion is the formation of insoluble salts or complex ions between anions in oxalic and sulfuric acids and calcium and aluminium ions leached from E-glass fibres. The property changes caused by humidity, temperature, and chemicals

on composites using propylene, vinyl ester, and polyester as matrix materials were examined by Xue et al. [39], Buck et al. [40], John and Naidu [41], and Singh et al. [42]. The bending properties and impact strength of glass fibre/epoxy composite after immersion in hydrochloric acid (HCl) and sodium hydroxide (NaOH) were analysed by Amaro et al. [43]. They reported that the impact strength, flexural strength, and flexural modulus decreased with exposure time; moreover, the alkaline solution significantly reduced the flexural properties more than the acid solution. Pai et al. [44, 45] revealed that the isophthalic polyester grade resin showed superior resistance to sulfuric acid, while the general-purpose polyester grade resin had relatively lower resistance. The effects of strong acids on the mechanical properties of glass/polyester composite pipes at average and high temperatures were investigated by Mahmoud and Tantawi [46]. It was carried out by exposing the composite pipes to four different acids: hydrochloric acid (HCl), sulfuric acid (H_2SO_4), nitric acid (HNO_3), and phosphoric acid (H_3PO_4) for up to 90 days. Aggressive acids have been found to have a variable effect on the specimens exposed at different temperatures. Flexural strength, hardness, and Charpy impact resistance variation depend on the type of acids and immersion time. It has also been noticed that sulfuric acid (H_2SO_4) has a more severe effect on the strength of composite pipes. All these studies have shown that acidic environments seriously affect the performance of composite materials depending on their types and concentrations. Although the acidic environment primarily deforms the matrix material, any cracks or surface defects during moulding or cooling cause the acid to reach the reinforcement material. The change in the properties of the reinforcement material, which has undertaken the task of strengthening the composite material, affects the properties of the material. However, it remains a fascinating subject; hence, the changes in the properties of composite materials exposed to environmental effects cannot be tied to specific rules. In using hybrid composite materials, the situation becomes more complex, and explaining the underlying causes of the hybrid effect mechanism becomes more difficult.

In this study, the changes in the absorptive, morphological, mechanical, structural, and thermal properties of glass-carbon fibre reinforced epoxy polymer (GCFREP) hybrid composite materials immersed in an acidic environment at different temperatures and varying exposure times are examined in detail. The results obtained are essential in revealing how the characteristic properties of GCFREP hybrid composite materials are affected by an acidic environment. The fact that all the data obtained are from experimental studies is due to the complexity of the event, the uncertainty of the behaviour both within and between layers, and the necessity of experimental data to make predictions and discuss the subject. Experimental studies carried out according to the standards and in sufficient quantities will significantly

contribute to converting physical facts into mathematical expressions and obtaining correct models. This study aims to fill this gap by examining the absorptive morphological, mechanical, structural and thermal properties of GCFREP hybrid composites.

Experimental

Materials, manufacturing, and specimen preparation

The materials used in the production process of hybrid composites are glass fabric, carbon fabric, and epoxy polymer. E-glass twill weave fabric with an areal density of 300 g/m² (supplied by Telateks Corporation (Manisa, Turkey)) and carbon 3 K twill weave fabric with an areal density of 245 g/m² (supplied by Telateks Corporation (Manisa, Turkey)) are used to reinforce the Araldite LY 1564 epoxy (supplied by Huntsman Corporation (Texas, USA)) cured with Aradur 3487 hardener. The mass ratio of epoxy polymer to hardener is 10:3.4 as per the specification of the manufacturer.

The vacuum-assisted resin-infusion method (VARIM) was applied to fabricate laminates with [G₂C]_s lay-up scheme, where C and G denote carbon and glass fibre, respectively. The resin mixture at room temperature was homogeneously impregnated into the GCFREP hybrid composite layers. The curing process for the impregnated plate was carried out by keeping the vacuum infusion table at 80 °C for 8 h and then at room temperature for 1 day [47]. E-glass and carbon fibre layers in the production of a hybrid composite plate (Fig. 1(a)) and a snapshot taken during the production process (Fig. 1(b)) are shown in Fig. 1. The dimensions of manufactured composites are 1000 mm x 1500 mm x 1.6 mm. The overall fibre weight fraction of the composites was approximately 66%. The composite laminates were cut into specimens with a CNC Router Machine for mechanical tests. The cleaning process with compressed air was carried out to remove the adhesion of the sawdust and dust particles on the specimen surface that emerged from the composite plates during the specimen-cutting process. The specimens used in mechanical characterisation tests are given in Fig. 2. In addition, the standards and dimensions of specimens cut for mechanical tests absorption are given in Table 1.

Environmental conditions

Experimental exposure environments consist of acidic solutions with a degree of acidity with pH 1.0 at -10, 25, and 40 °C. Tensile, compression, three-point bending, Charpy impact, and absorption specimens were stored in 12 different exposure environments for varying periods of

1 day and 1–3–6–9–12 weeks. The schematic representation of the experimental parameters is given in Fig. 3.

The simulated acidic rain was prepared by adjusting the pH to 1.0 using a 5:1 mixture of concentrated sulfuric acid (H₂SO₄) and nitric acid (HNO₃). Efforts were made to maintain pH control by conducting daily pH measurements. If the pH value increased, an acid mixture was added; conversely, in the event of a decrease, distilled water was added to maintain a pH of at least 1.0 ± 0.1 [48].

While an exposure environment at -10 °C was provided by using the deep freezer of the refrigerator, exposure environments at 25 and 40 °C were provided with the help of magnetic stirrer heaters. The experimental acidic immersion environments can be seen in Fig. 4. Hybrid composite specimens, kept in an acidic environment for the specified time, were removed from the acid baths, dried and kept at room temperature for 24 h. Further characterisations were carried out with the dried specimens.

Characterisation

Absorptive properties

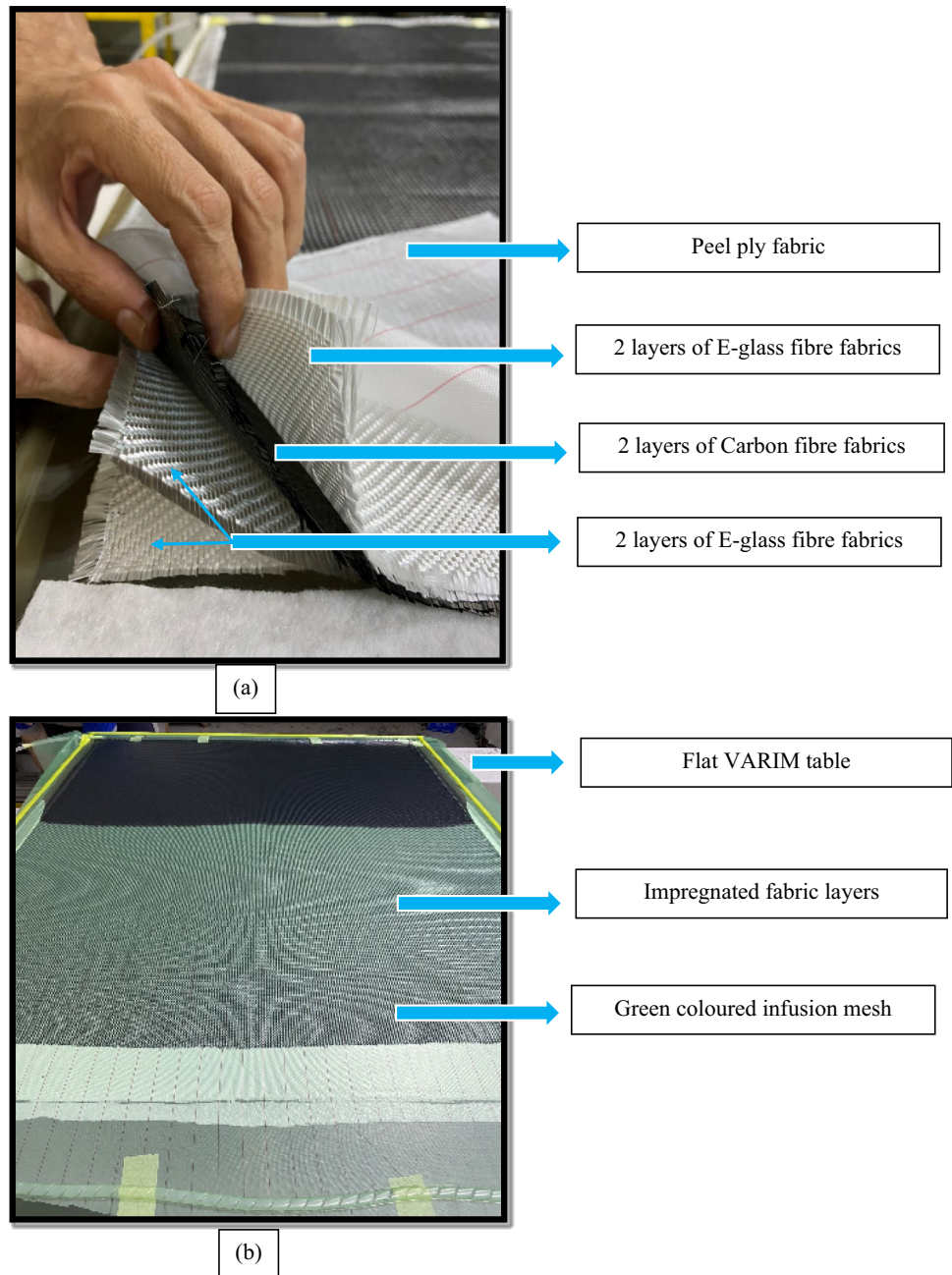
The weights of the marked absorption specimens were recorded before they were exposed to the acidic environment. In addition, the characteristic moisture absorption data of the GCFREP hybrid composite were obtained by measuring the weights of these specimens at the end of the determined periodic exposure times (achieved by removing surface moisture with a dry cloth and keeping them for 1 day at room temperature). The weights of five specimens were measured, with each weight being measured three times using a Radwag AS 220/C/2 brand analytical balance with a resolution of 0.0001 g. Weight variation was calculated by using Eq. (1):

$$\begin{aligned} \text{Change in weight, \%} \\ = \frac{\text{weight after absorption} - \text{weight before absorption}}{\text{weight before absorption}} \times 100 \end{aligned} \quad (1)$$

Morphological properties

The morphology of the GCFREP hybrid composites was analysed using a scanning electron microscope (SEM, Carl Zeiss 300VP). In order to obtain surface micrographs, a 15 kV acceleration voltage was used in accordance with the E986 standard. Prior to analysis, the specimens were coated with 5 nm gold under vacuum via the ion sputter coater. In addition to that, the surface characterisation of absorption test specimens was examined under an optical microscope (Nikon LV150N).

Fig. 1 **a** E-glass-carbon weave fabrics and **b** production of the hybrid composite

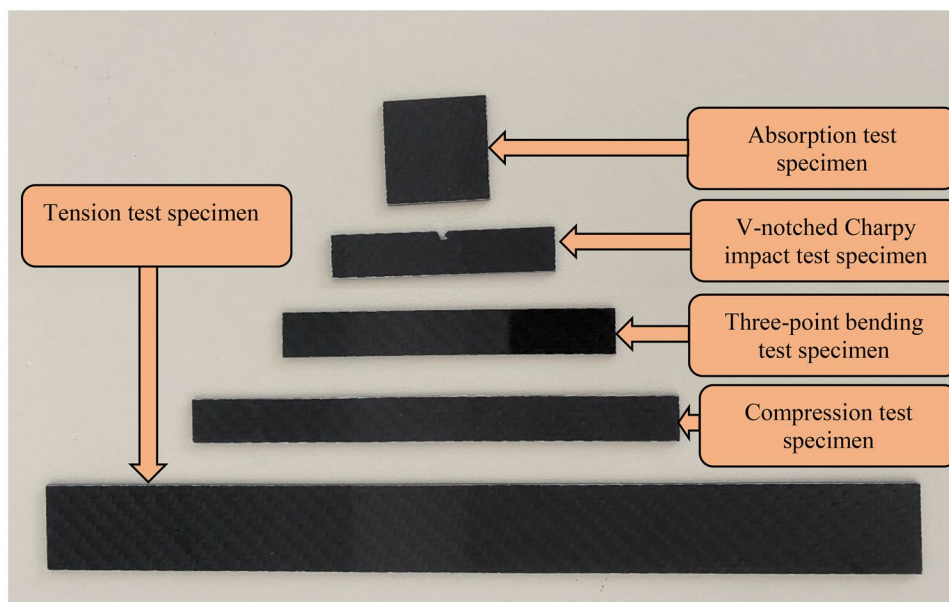


Mechanical properties

Mechanical characterisation of GCFREP hybrid composites exposed to different experimental environments at specified times and temperatures was performed by tensile, compression, three-point bending, and Charpy impact tests. In order to minimise experimental errors, five trials were performed for each parameter, and the average values were recorded as test results.

Tensile, compression, and three-point bending tests were performed at room temperature at a rate of 1 mm/

min using a Shimadzu 100 kN device in accordance with ASTM standards listed in Table 1. Tensile tests were performed to determine the tensile strength, Young's modulus, and tensile stress; compression tests were performed to determine the compressive strength, strains at maximum compressive stress, and compressive modulus; three-point bending tests were performed to determine the maximum flexural strain and flexural modulus; and V-notch Charpy impact tests were performed to determine varying impact strength of GCFREP hybrid composites.

Fig. 2 Mechanical characterisation test specimens

Structural properties

Fourier transform infrared spectroscopy (FTIR) was used to determine the functional groups of the GCFREP hybrid composites aged in an acidic environment. FTIR spectra of hybrid composites were obtained using a Perkin Elmer Spectrum Two with a spectral resolution of 4 cm^{-1} . The spectrometer was equipped with a diamond/ZnSe ATR (Attenuated Total Reflection) accessory. Before the measurements, a thin layer was cut from the corners of the epoxy composites exposed to absorption. Data acquisition was performed automatically using a computer with Spectrum™ 10 software.

Thermal properties

The thermal properties of the GCFREP hybrid composites were examined by thermogravimetric analysis (TGA) and differential scanning calorimetry (DSC). The specimens

(~10–20 mg in a platinum pan) were investigated using the TA TGASDT Q600 and DSC-TA Q10 thermal analysers with a ramp rate of $10\text{ }^{\circ}\text{C}/\text{min}$.

Results and discussion

The ageing effects of an acidic environment were investigated on the absorptive, morphological, mechanical, structural, and thermal properties of GCFREP hybrid composites aged at pH 1.0 at different temperatures and time intervals.

Absorptive properties

In order to illustrate the typical diffusion properties of hybrid composite specimens, the percentage of weight gain during moisture absorption is shown in Fig. 5 as a function of exposure time. Each experimental point represents the average of three measurements on individual specimens.

Table 1 Standards and specimen sizes used for mechanical characterisation tests

Test	Standard	Dimension (mm × mm)
Tension	ASTM D3039—Standard Test Method for Tensile Properties of Polymer Matrix Composite Materials	250 × 25
Compression	ASTM D3410—Standard Test Method for Compressive Properties of Polymer Matrix Composite Materials with Unsupported Gage Section by Shear Loading	140 × 12.7
Three-point bending	ASTM D7264—Standard Test Method for Flexural Properties of Polymer Matrix Composite Materials	96 × 13
V notched Charpy impact test	ASTM D256 – Standard Test Methods for Determining the Charpy Pendulum Impact Resistance of Plastics	65 × 12.7
Absorption	ASTM D2734—Standard Test Methods for Void Content of Reinforced Plastics	30 × 30

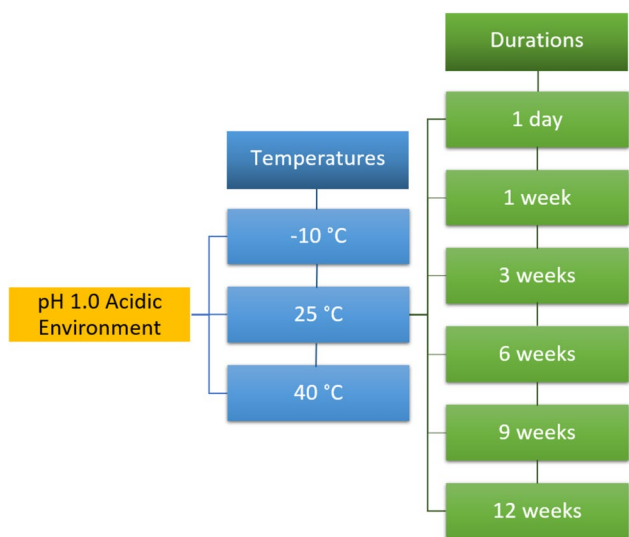


Fig. 3 The schematic representation of the experimental parameters

The moisture absorption curves reveal a pseudo-Fickian behaviour in which the weight gain gradually increases with prolonged immersion time; notably, the pattern does not reach an equilibrium as postulated by Weitsman and Barjasteh [49, 50].

The absorption capacity of the specimens is quite strong in the acidic solution at 40 °C, followed by that at 25 °C, and weak in the acidic solution at -10 °C. In other words, an increase in the acidic ambient temperature increases the moisture absorption rate. This is because the increased temperature accelerates the degradation process in the epoxy resin, and as a result, the porosity and liquid uptake of the specimens increases [51]. The increase in initial high

moisture absorption rate slowed after the sixth week, and partial saturation set in for specimens immersed in an acidic environment at 40 °C. These specimens absorb the maximum amount of moisture of 8%. However, for the specimens kept at 25 °C, the absorption rate slowed down after the ninth week. The highest moisture contents of 7% were observed at 12 weeks under 25 °C conditions. The specimens at a lower temperature of -10 °C continue to gain weight throughout the exposure time with maximum moisture contents of 0.66% at 12 weeks. This implies that the moisture absorption rate is very low for the specimens under -10 °C conditions. The diffusion accelerating effect of temperature is approximately 13.16 times greater at 40 °C and 11.67 times greater at 25 °C compared to the situation at -10 °C. This indicates that specimens exposed to an acidic environment at -10 °C exhibit much better chemical resistance than specimens exposed to acidic environments at higher temperatures.

An increase in the overall weight of the specimen can be attributed to the penetration of acid solution in the specimen during immersion. However, a slight decrease in sample weight can occur when soluble compounds are leached into the acidic solution. The presence of voids or cracks in the matrix as well as fibre–matrix interface, can expedite the weight gain/loss effect in the materials [47].

Morphological properties

In order to identify the damage on the specimen surfaces and to present the micro damage morphology in the failure regions, optical microscope and SEM observations were performed on GCFREP hybrid composites immersed in an

Fig. 4 Experimental pH 1.0 acid exposure environments at -10 and 40 °C

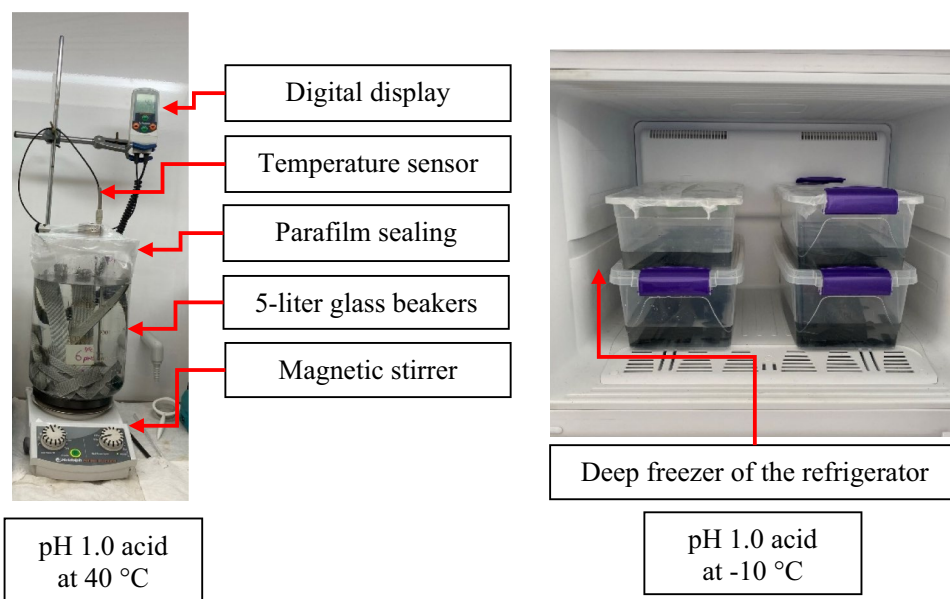


Fig. 5 Weight gain as a function of duration for GCFREP hybrid composites after exposure to acidic environment at temperatures of -10, 25, and 40 °C

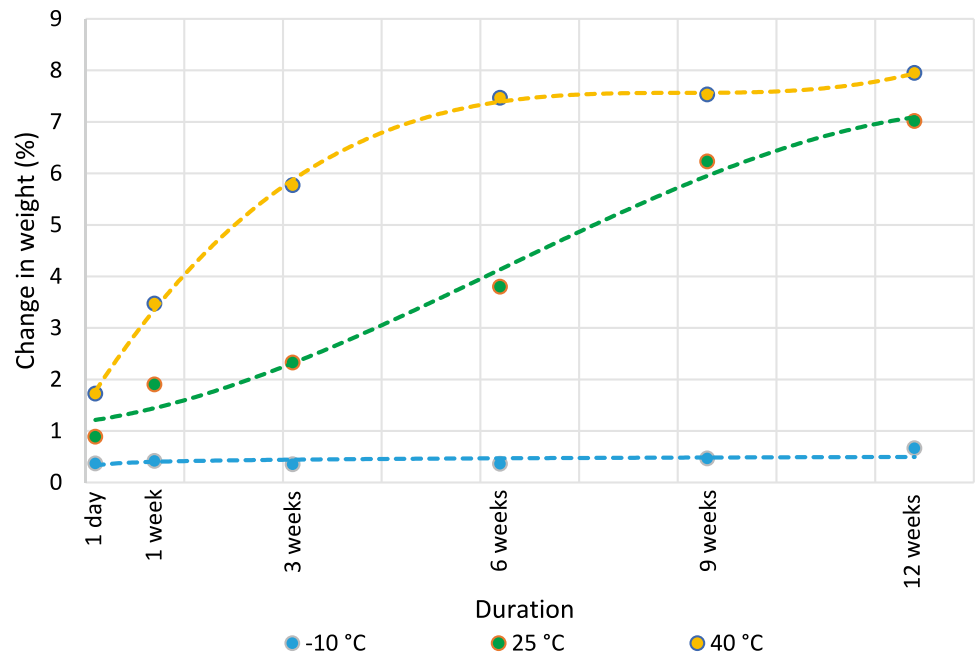


Table 2 Optical microscope images of the specimen surfaces before and after ageing

Temperature / Duration	Raw	-10 °C	25 °C	40 °C
1 day				
1 week				
3 weeks				
6 weeks				
9 weeks				
12 weeks				

acidic environment with a pH of 1.0 for various exposure times and temperatures. Table 2 shows the optical microscopy images of the specimen surfaces of the hybrid composites after 12 weeks of exposure.

Table 2 shows that the surface of the raw (non-aged) specimen is smooth compared to the surfaces of the specimens kept in acidic environments. As the ageing duration increases, the surfaces of the specimens are no longer smooth, and voids become evident. These surface changes are caused by leaching of soluble compounds into the acidic solution. Colour changes can also be observed typically caused by degradation and oxidation of the epoxy resin and the pigments or fillers used in the composite material [52]. No significant difference was observed in the colour of the specimens cooled at $-10\text{ }^{\circ}\text{C}$ compared to those at 20 and $40\text{ }^{\circ}\text{C}$. Although the surface colour of specimens cooled at $-10\text{ }^{\circ}\text{C}$ changed from black to grey after 12 weeks of acid exposure, the surface colour of specimens under the same conditions remained almost unchanged for up to 3 weeks, resulting in slight discolouration. The most severe colour change was detected for the specimens immersed in an acidic environment of $40\text{ }^{\circ}\text{C}$. The surface colour of the specimens under $40\text{ }^{\circ}\text{C}$ condition changed from black to yellow after 12 weeks of acid exposure. Moreover, the acidic environment of $40\text{ }^{\circ}\text{C}$ has a more significant effect on the gloss loss of the specimens over 12 weeks.

SEM micrographs of the specimens kept in an acidic environment with a pH of 1.0 at -10 , 25 , and $40\text{ }^{\circ}\text{C}$ for 1, 6, and 12 weeks are shown in Fig. 6. Some markers were used

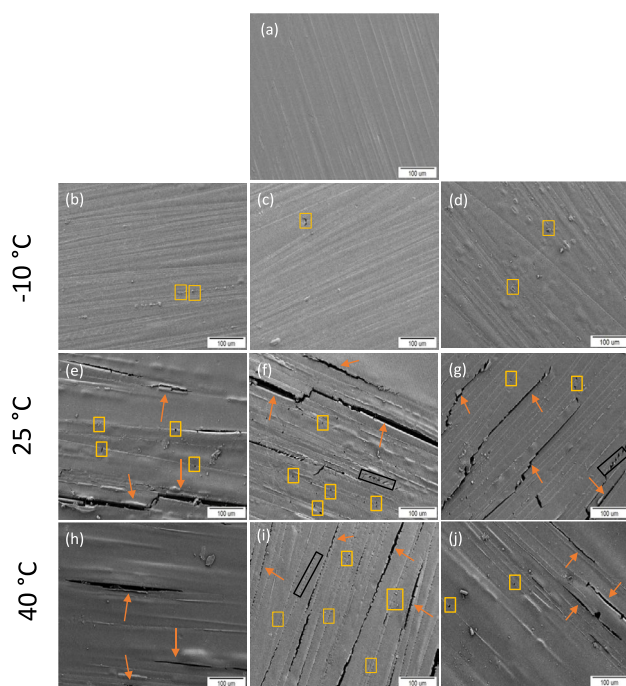


Fig. 6 SEM micrographs of the **a** control specimen and specimens stored for **b-h** 1 week, **c-i** 6 weeks, and **d-j** 12 weeks in an acidic environment at different temperatures

to raise awareness. Micro-cracks and micro-voids are represented by an orange arrow sign and a yellow rectangular marker, respectively. Acid attacks start from the surface of the specimens in the first week. Due to the sensitivity of the epoxy resin to the acidic environment, the hybrid composites are affected, leading to the emergence of matrix microcracks and microvoids on the specimen surfaces. These deformations become more pronounced as the acidic ambient temperature and duration of acid exposure increase.

Mechanical properties

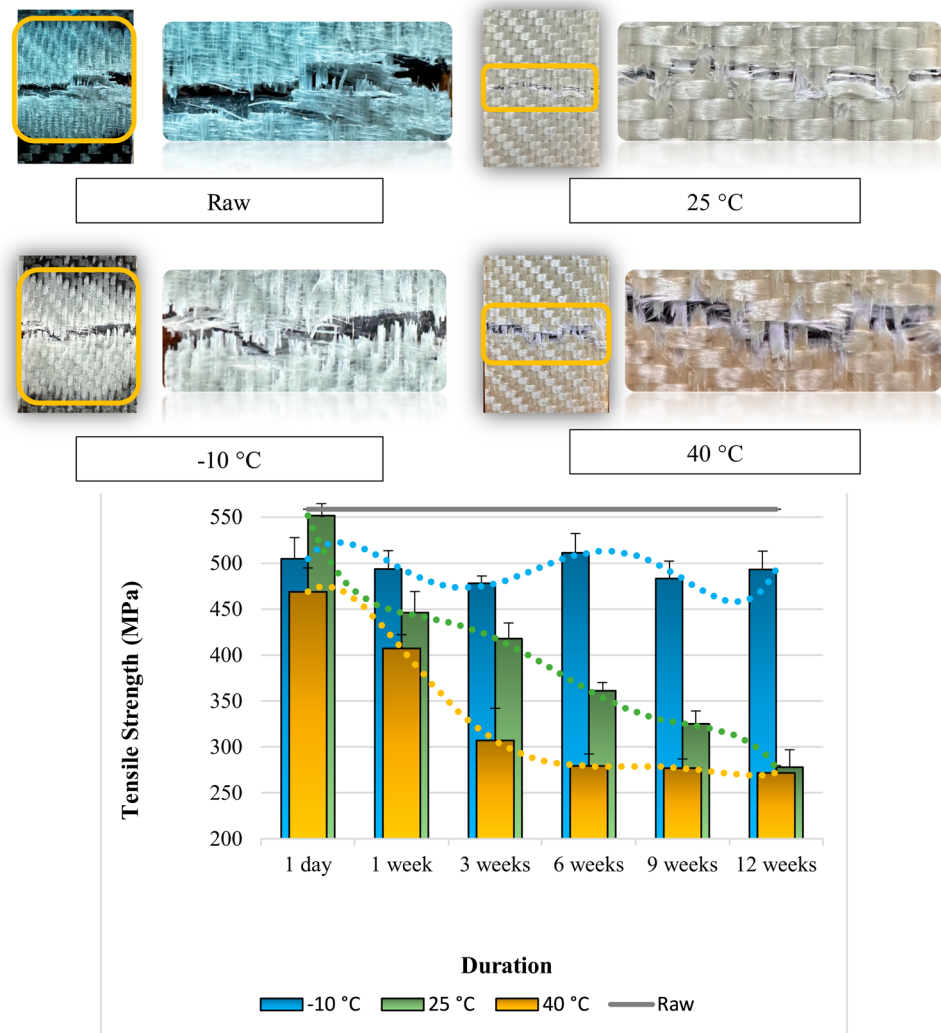
Tensile tests

The tensile strengths with trend lines of GCFREP hybrid composites immersed in an acidic environment with pH 1.0 at three different temperatures for exposure times up to 12 weeks and the corresponding failure modes after 12 weeks are given in Fig. 7. In addition, the values for tensile strength, strain at tensile strength, and Young's modulus are given in Table 3. In Table 3, the up-down trends of the specimens compared to the raw specimen data are indicated with arrows along with the percentage change.

Firstly, it should be noted that there are differences between the failure modes. When the tensile stresses due to axial loading exceed the tensile strength of the hybrid composite, failure of the composite occurs. The photographs show that the acidic ambient temperatures at which the hybrid composites are aged change their tensile failure modes. Similar to the behaviour of raw specimens, specimens kept at low temperatures in an acidic environment rupture in a brittle manner through the horizontal axis without warning before final failure, while specimens fail in a ductile manner at higher temperatures. In addition, E-glass fibres in the outermost layers are revealed in the GCFREP hybrid composite laminates with $[\text{G}_2\text{C}]_s$ orientation due to the degradation of the outermost layer epoxy of the specimens exposed to a pH 1.0 acidic environment at 25 and $40\text{ }^{\circ}\text{C}$. The browning/darkening effect caused by exposure to the pH 1.0 acidic environment at $40\text{ }^{\circ}\text{C}$ reduces the failure mode conspicuity of E-glass fibres.

When evaluated in terms of tensile strength, it has been observed that the specimens exposed to all conditions of pH 1.0 acidic environment are lower than that of the raw specimens. In addition, the effects of temperatures on tensile strength are found to be different. Increasing temperatures have an increasing impact on the tensile strength of the GCFREP hybrid composites. A clear change trend in tensile strength is not observed for specimens kept at $-10\text{ }^{\circ}\text{C}$, where only a tiny amount of moisture absorption was experienced during ageing. As seen in Fig. 6, voids and cracks in the resin caused by moisture penetration are rare in an acidic environment at $-10\text{ }^{\circ}\text{C}$. It has been revealed that the

Fig. 7 Failure modes of 12 weeks acid-exposure and tensile strength – strain graph for GCFREP hybrid composites



tensile strength of the specimens kept at 25 °C decreases with the prolonged exposure times, and the specimens with the lowest values are those of that were kept for 12 weeks, which was the longest experimental exposure time. This decrease is caused by partial interfacial debonding between the fibre and the resin due to the hydrolysis reaction of the epoxy resin [53]. The tensile strength of the specimens kept at 40 °C shows a rapid decrease during the initial ageing period, and this deterioration gradually slows down with the prolongation of the ageing period. The rapid degradation observed in the first 3 weeks is due to delamination and separation of the fibre/matrix interface bond caused by swelling of the moisture absorption, corresponding to the Fickian diffusion process in Fig. 5. However, the slower degradation after three weeks of ageing could be attributed to the polymer of composites relaxation, as Li et al. pointed out [54]. The strength of specimens at 40 °C remains constant at about 279 MPa after 6 weeks of ageing. The tensile strength of specimens exposed to an acidic environment with

a pH of 1.0 for 12 weeks at 40 °C has decreased by 51.4%, and that of the specimens stored at 25 °C for 12 weeks has decreased by 50.2%. Similar to the tensile strength, the tensile strains of the specimens at 25 and 40 °C mostly decrease with increasing acid exposure time. The strain values of the specimens exposed to an acidic environment with a pH of 1.0 at 25 and 40 °C for 12 weeks have decreased by 50.0% and 55.6%, respectively, compared to the values of the raw specimens. The decreased failure strain can pose a risk to the service reliability of the hybrid composite. However, the strain values of the specimens held at -10 °C have always been found higher than that of the raw specimen. At the end of the 12 weeks, the maximum tensile strain is 1.25 times higher than that of the raw specimen. This may be attributed to the lower decomposition at low temperatures. The scattering seen in results for strains does not allow clear and conclusive conclusions regarding the mechanisms of chemical ageing. The modulus of elasticity of hybrid composites tends to decrease with exposure time, it is generally seen that acid

Table 3 Tensile strength, Tensile strain, and Young's modulus of raw and acid-exposure GCFREP hybrid composites

Raw	Tensile strength (MPa)			Strain at Tensile Strength (%)			Young's Modulus (GPa)		
	558.3 (± 17.4)			1.8 (± 0.2)			38.4 (± 4.9)		
Temperature/ Duration	-10 °C	25 °C	40 °C	-10 °C	25 °C	40 °C	-10 °C	25 °C	40 °C
1 day	504.7 (± 23.6) -9.6%↓	551.3 (± 13.2) -1.3%↓	468.7 (± 26.3) -16.0%↓	2.2 (± 0.4) 22.2%↑	1.6 (± 0.1) -11.1%↓	2.5 (± 0.4) 38.9%↑	24.9 (± 1.6) -35.2%↓	38.4 (± 3.6) 0.0%↓	31.6 (± 3.1) -17.7%↓
1 week	493.5 (± 20.0) -11.6%↓	446.1 (± 23.7) -20.1%↓	407.1 (± 15.1) -27.1%↓	2.1 (± 0.5) 16.7%↑	1.7 (± 0.5) -5.6%↓	2.5 (± 0.5) 38.9%↑	36.7 (± 1.3) -4.4%↓	34.9 (± 8.2) -9.1%↓	30.2 (± 7.9) -21.4%↓
3 weeks	478.0 (± 8.6) -14.4%↓	417.8 (± 17.3) -25.2%↓	306.9 (± 35.9) -45.0%↓	1.4 (± 0.3) -22.2%↓	2.0 (± 1.4) 11.1%↑	1.2 (± 0.2) -33.3%↓	25.5 (± 6.6) -33.6%↓	23.1 (± 8.6) -39.8%↓	29.7 (± 0.7) -22.7%↓
6 weeks	511.2 (± 21.8) -8.4%↓	361.1 (± 9.1) -35.3%↓	279.2 (± 13.8) -50.0%↓	2.1 (± 0.4) 16.7%↑	1.9 (± 0.3) 5.6%↑	1.5 (± 0.4) -16.7%↓	22.3 (± 4.2) -41.9%↓	24.7 (± 7.5) -35.7%↓	29.1 (± 4.1) -24.2%↓
9 weeks	483.2 (± 19.2) -13.5%↓	325.1 (± 14.1) -41.8%↓	276.9 (± 10.4) -50.4%↓	2.6 (± 1.0) 44.4%↑	1.0 (± 0.1) -44.4%↓	1.3 (± 0.1) -27.8%↓	18.7 (± 0.2) -51.3%↓	22.5 (± 2.4) -41.4%↓	28.3 (± 2.5) -26.3%↓
12 weeks	493.1 (± 20.9) -11.7%↓	277.9 (± 19.8) -50.2%↓	271.6 (± 8.4) -51.4%↓	2.3 (± 0.2) 27.8%↑	0.9 (± 0.1) -50.0%↓	0.8 (± 0.2) -55.6%↓	22.9 (± 4.9) -40.4%↓	21.4 (± 0.5) -44.3%↓	28.6 (± 6.9) -25.5%↓

exposure causes a decrease in the stiffness. At the end of 12 weeks, the decrease in Young's modulus is approximately 25–40%. Young's modulus reduces from 38.4 GPa to 22.9 GPa, 21.4 GPa, and 28.6 GPa for specimens exposed to an acidic environment at -10, 25, and 40 °C, respectively.

Compression tests

The values of compressive strength, compressive strain at failure, compression modulus, and failure modes through the thickness and in-plane of GCFREP hybrid composites as a result of compression tests are given in Fig. 8 and Table 4. In compression, while fibre crushing is observed in the raw specimen and specimens at -10 °C, the formation of in-plane kink bands [55] was observed in specimens at 25 and 40 °C conditions. In the literature, fibre crushing failure and kink formation are reported as the most common failures of fibre-reinforced polymer composites [56]. Fibre crushing failure is defined as damage that occurs when the compressive stress applied to the composite exceeds the intrinsic crushing strength of the fibres [57], while kinking is defined as a localised deformation in a band across the composite in which the fibres exhibit rotation and the matrix material undergoes severe shear deformation [55].

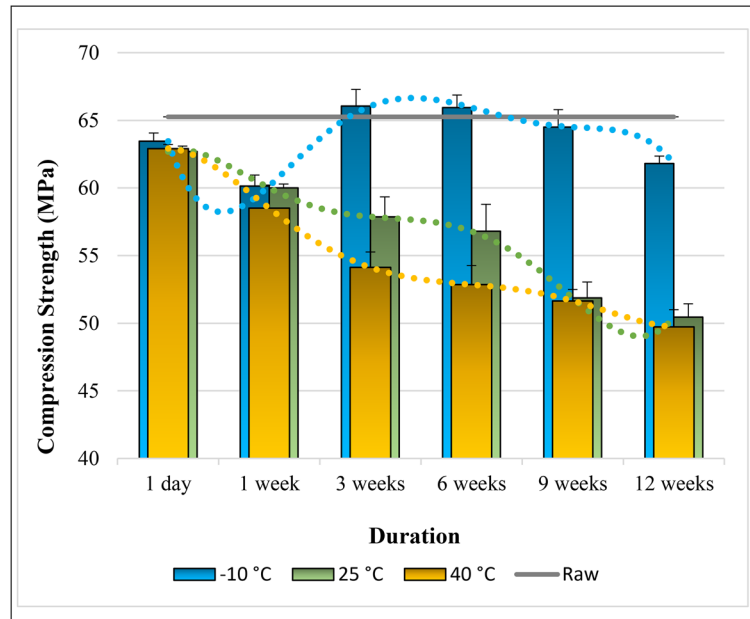
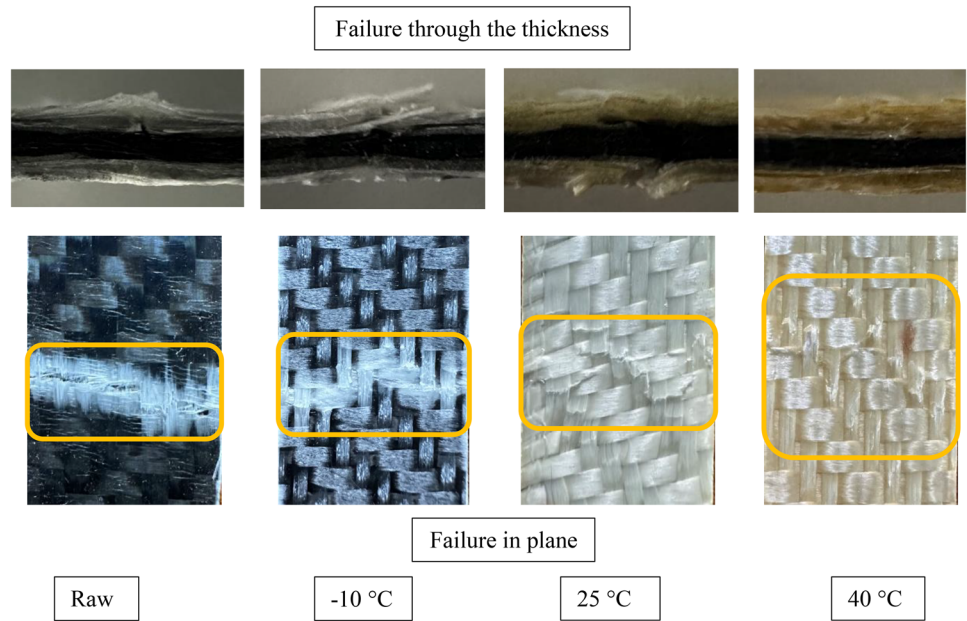
Similar to the effect of an acidic environment on the tensile strength of GCFREP hybrid composites, increasing temperatures also significantly reduce the compressive strength of these composites. Due to the ductility of the polymers at high temperatures, lower compressive strength at higher temperatures is expected. The decrease in compressive strength of the specimens stored at 40 °C for 12 weeks is

23.9% compared to that of the raw specimen. Hybrid composites stored at 25 °C show similar performance at compression loading. However, the situation is reversed for the specimens exposed to an acidic environment at -10 °C. The compressive strength of the specimens stored at -10 °C for 3 and 6 weeks is higher than that of the raw specimen due to their brittle behaviour. The decrease in the compressive strength of the hybrid composites in the first week can be explained by the absorption of acidic solution, while their high chemical degradation can explain the decrease seen in the 12th week. The highest value for the compressive strength of the specimens stored under the specified conditions was found to be 66.1 MPa for the specimens stored at -10 °C for 3 weeks, and the lowest compressive strength was found to be 49.7 MPa for the specimens stored at 40 °C for 12 weeks. Compared with the raw specimen, the maximum increase in compressive strength is 1.2%, while the maximum decrease in compressive strength is 23.9%.

When the compressive strain values are examined, it is seen that acid exposure time increases the compressive strain in the first weeks and decreases it for high-temperature environments in the later period. The increase in strain in the first week can be explained by the ductility of the material due to acid absorption.

The general trend in compression modulus is a decrease with increasing temperature and acid exposure time. It shows its lowest value of 3.9 GPa at 40 °C in the 12th week. At the end of 12 weeks, the compressive modulus value decreased by 17.0%, 22.6%, and 26.4%, respectively, at -10, 25, and 40 °C relative to the raw specimen. After the ninth week, the sharp decrease in the compression modulus decreased.

Fig. 8 Failure modes of 12 weeks acid-exposure and compression strength – duration graph for GCFREP hybrid composites



Three-point bending tests

The flexural strengths, strain to failure, and flexural modulus of the specimens, which were kept for 12 weeks in an acidic environment with pH 1.0 as a result of the three-point bending tests, are listed in Table 5 and shown graphically in Fig. 9. As can be seen from the results, the bending properties of hybrid composites decrease with the increase of the acidic ambient temperature and exposure time in an acidic environment.

The tendency to change in flexural strength of hybrid composites due to acidic ambient temperature and exposure time in an acidic environment is similar to that of tensile

strengths. The increased absorption of acidic solution at high temperatures increased the sensitivity of the mechanical responses of the hybrid composites.

Figure 9 shows the strong influence of increasing temperature on the flexural strength of the specimens. Even keeping the specimen in an acidic environment for 1 day caused poor bending performance. While the flexural strength of the specimens exposed to the acidic environment at 40 and 25 °C tended to decrease with a trend related to their moisture absorption behaviours as the exposure time increased, no significant change in the flexural strength is observed for the specimens kept at -10 °C. This indicates that a weight

Table 4 Compression strength, strain, and modulus of raw and acid-exposure GCFREP hybrid composites

Raw	Compression strength (MPa)			Strain (%)			Compression Modulus (GPa)		
	65.3 (± 2.1)			2.4 (± 0.2)			5.3 (± 4.9)		
Temperature / Duration	-10 °C	25 °C	40 °C	-10 °C	25 °C	40 °C	-10 °C	25 °C	40 °C
1 day	63.5 (±0.6) -2.8%↓	62.7 (±0.4) -4.0%↓	62.9 (±0.3) -3.7%↓	2.2 (±0.1) -8.3%↓	2.5 (±0.4) 4.2%↑	2.6 (±0.2) 8.3%↑	5.1 (±0.3) -3.8%↓	5.2 (±0.7) -1.9%↓	5.3 (±0.2) 0%↔
1 week	60.1 (±0.8) -8.0%↓	60.00 (±0.3) -8.1%↓	58.5 (±1.7) -10.4%↓	2.1 (±0.2) -12.5%↓	1.8 (±0.7) -25.0%↓	2.8 (±0.5) 16.7%↑	5.3 (±0.4) 0.0%↔	5.2 (±0.6) -1.9%↓	4.3 (±0.3) -18.9%↓
3 weeks	66.1 (±1.2) 1.2%↑	57.9 (±1.5) -11.3%↓	54.1 (±1.1) -17.2%↓	2.4 (±0.4) 0.0%↔	2.0 (±0.5) -16.7%↓	1.4 (±0.2) -41.7%↓	5.2 (±0.1) -1.9%↓	4.5 (±0.1) -15.1%↓	4.7 (±0.3) -11.3%↓
6 weeks	65.9 (±0.9) 0.9%↑	56.8 (±2.0) -13.0%↓	52.9 (±1.4) -19.0%↓	2.9 (±0.4) 20.8%↑	1.7 (±0.1) -29.2%↓	1.5 (±0.1) -37.5%↓	4.6 (±0.1) -13.2%↓	4.3 (±0.1) -18.9%↓	4.1 (±0.1) -22.6%↓
9 weeks	64.5 (±1.3) -1.2%↓	51.9 (±1.2) -20.5%↓	51.7 (±0.8) -20.8%↓	2.8 (±0.2) 16.7%↑	1.6 (±0.1) -33.3%↓	1.4 (±0.1) -41.7%	4.3 (±0.1) -18.9%↓	4.2 (±0.1) -20.8%↓	3.9 (±0.1) -26.4%↓
12 weeks	61.8 (±0.5) -5.4%↓	50.4 (±1.0) -22.8%↓	49.7 (±1.3) -23.9%↓	2.8 (±0.6) 16.7%↑	1.6 (±0.2) -33.3%↓	1.6 (±0.1) -33.3%↓	4.4 (±0.1) -17.0%↓	4.1 (±0.2) -22.6%↓	3.9 (±0.2) -26.4%↓

change may indicate a change in flexural strength. The lowest bending strength was observed in the specimens kept at 40 °C for 12 weeks. The decrease in the flexural strength of these specimens is 75.0% compared to that of the raw specimens, while it is 16.7% for the specimens kept at -10 °C. This situation can be explained by the higher degradation rate associated with the poor fibre-matrix interface due to the high moisture absorption at high acidic ambient temperatures. On the other hand, the reduction in flexural strength and flexural modulus caused by acid exposure of hybrid composites compared to that of raw samples can be attributed to swelling and deterioration of the matrix. A greater property reduction is observed with increasing immersion time and acidic ambient temperature. This reduction is

maximum in specimens kept in an acidic environment for 12 weeks and is 38.2% for flexural strain and 73.9% for flexural modulus. When the flexural strain changes due to acid exposure time are compared, it is noted that the flexural strains of hybrid composites increase until partial saturation. The increase in flexural strain can be attributed to the flexible structure resulting from the absorption of solvent molecules filling the voids and cracks in the hybrid composite and acting as plasticisers in the composite.

After bending testing, compression failure is observed at the upper surface of the specimens and tensile failure at the lower surface. In compression, macrocracks and localised kink bands are evident, extending across the entire width of the specimen. Kinking, the most predominant

Table 5 Flexural strength, strain, and modulus of raw and acid-exposure GCFREP hybrid composites

Raw	Flexural Strength (MPa)			Flexural Strain (%)			Flexural Modulus (GPa)		
	915.3 (± 15.7)			3.4 (± 0.1)			35.2 (± 0.5)		
Temperature / Duration	-10 °C	25 °C	40 °C	-10 °C	25 °C	40 °C	-10 °C	25 °C	40 °C
1 day	721.2 (±7.3) -21.2%↓	719.0 (±43.2) -21.4%↓	592.7 (±26.1) -35.2%↓	2.7 (±0.1) -20.6%↓	2.7 (±0.1) -20.6%↓	2.6 (±0.2) -23.5%↓	24.7 (±1.1) -29.8%↓	28.1 (±4.2) -20.2%↓	28.3 (±4.2) -19.6%↓
1 week	769.8 (±32.0) -15.9%↓	562.6 (±28.2) -38.5%↓	408.4 (±17.5) -55.4%↓	2.7 (±0.1) -20.6%↓	2.5 (±0.1) -26.5%↓	3.1 (±0.7) -8.8%↓	31.8 (±1.7) -9.7%↓	23.6 (±3.0) -33.0%↓	19.4 (±2.1) -44.9%↓
3 weeks	777.9 (±38.0) -15.0%↓	450.6 (±29.1) -50.8%↓	282.6 (±10.5) -69.1%↓	2.8 (±0.1) -17.6%↓	2.7 (±0.1) -20.6%↓	2.9 (±0.6) -14.7%↓	30.0 (±2.5) -14.8%↓	15.9 (±1.5) -54.8%↓	13.5 (±1.1) -61.6%↓
6 weeks	787.5 (±19.0) -14.0%↓	388.5 (±12.5) -57.6%↓	234.5 (±25.4) -74.4%↓	2.9 (±0.1) -14.7%↓	3.0 (±0.2) -11.8%↓	2.1 (±0.2) -38.2%↓	33.5 (±2.9) -4.8%↓	15.2 (±1.6) -56.8%↓	12.4 (±2.0) -64.8%↓
9 weeks	752.4 (±37.4) -17.8%↓	266.0 (±10.0) -70.9%↓	245.1 (±4.1) -73.2%↓	2.9 (±0.1) -14.7%↓	2.2 (±0.6) -35.3%↓	1.9 (±0.2) -44.1%↓	26.1 (±3.9) -25.9%↓	13.0 (±2.5) -63.1%↓	10.5 (±1.7) -70.2%↓
12 weeks	762.8 (±46.1) -16.7%↓	229.9 (±13.9) -74.9%↓	229.2 (±19.7) -75.0%↓	2.9 (±0.1) -14.7%↓	2.7 (±0.2) -20.6%↓	2.1 (±0.1) -38.2%↓	31.5 (±2.1) -10.5%↓	9.2 (±2.1) -73.9%↓	9.3 (±1.8) -73.6%↓

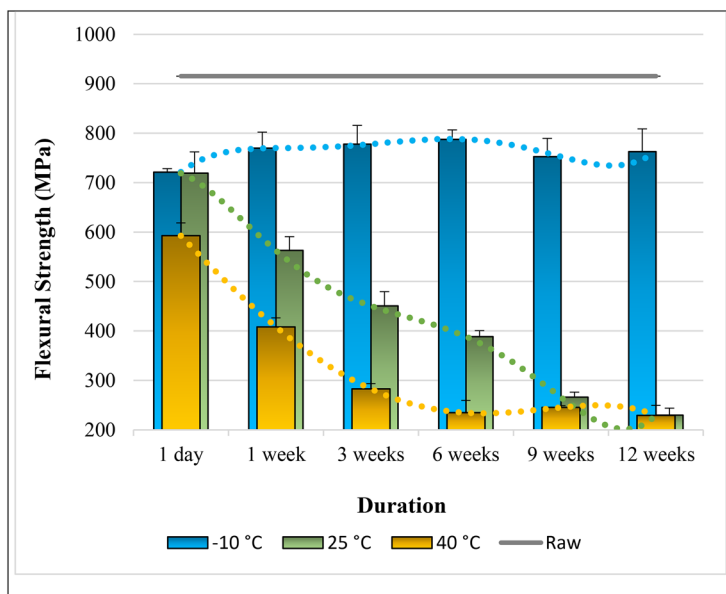
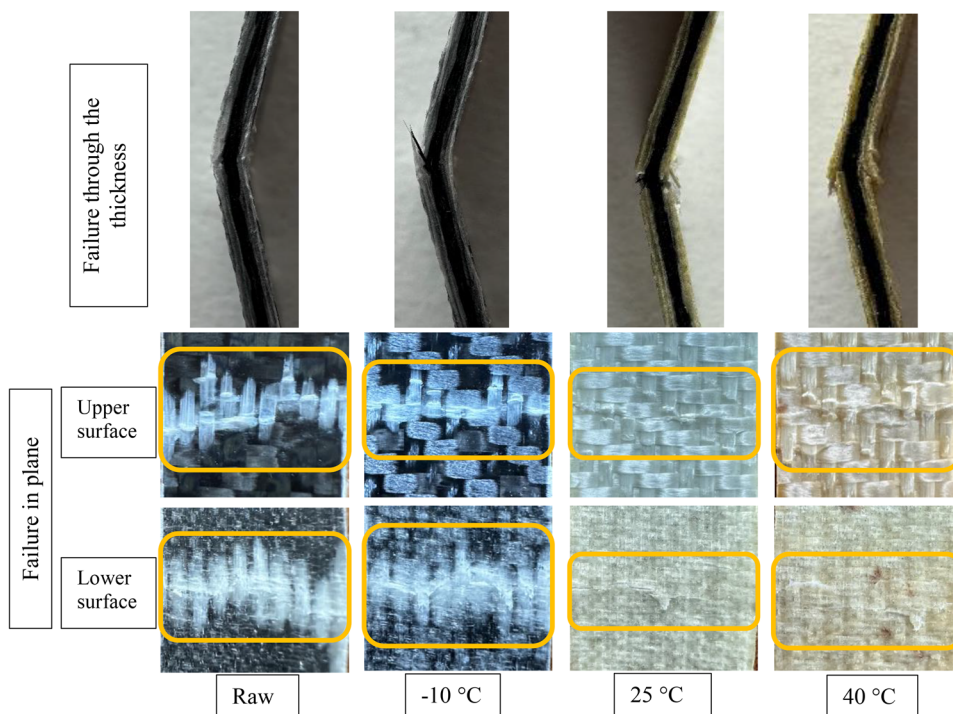
form of compressive failure, is also reported by Bonsu et al. [58] and Dong et al. [59]. Figure 8 shows that the damage at -10 °C is more pronounced than the failure at 40 °C, although it exhibits higher bending strength.

V-notched charpy impact tests

As a final test of mechanical characterisation, Charpy tests were performed to examine the energy absorption capacity of the hybrid composites. The fracture energy values found as a result of the V-notch Charpy impact test are given in

Fig. 10 with the standard deviation and listed in Table 6. The first implication from the graph is that exposure to an acidic environment decreased the fracture toughness of the hybrid composites. The negative effect on the fracture toughness of the specimens kept at 25 and 40 °C is more pronounced than those kept at -10 °C. The fracture toughness of the composites is affected by the ambient temperature to which the specimens are exposed rather than the acid exposure time. Contrary to expectations, no increase in fracture toughness is observed with increasing acidic ambient temperature. However, with the increase in the acid exposure time,

Fig. 9 Failure modes of 12 weeks acid-exposure and flexural strength – duration graph GCFREP hybrid composites



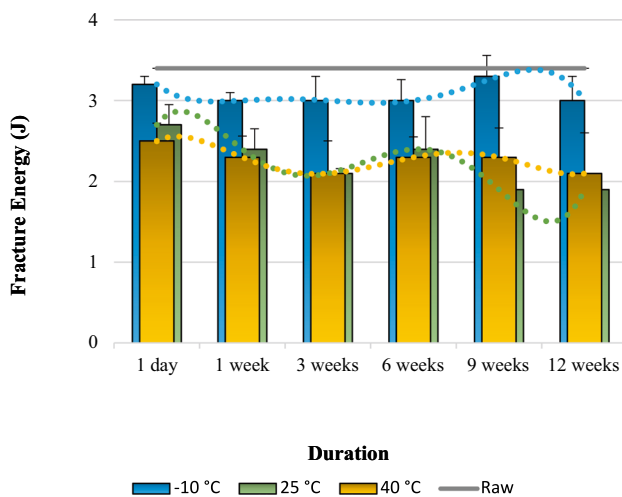


Fig. 10 Fracture energy – duration graph of raw and acid-exposure GCFREP hybrid composites

fluctuations are seen in fracture energy values. The fracture energy of the specimens after 12-week ageing is 3.0, 1.9, and 2.1 J for specimens exposed to the acidic ambient temperature of -10, 25, and 40 °C, respectively. Local heterogeneities in both microstructure and interfacial quality between laminates with different properties may be the reason for this situation.

Exposure to an acidic environment at different temperatures and prolonged periods causes different degradation rates in the matrix, resulting in differences in hybrid composite matrix behaviour. Accordingly, different behavioural tendencies are observed in fracture energy values. The matrix and fibre thermal coefficient differences of the specimens exposed to the acidic environment at different temperatures cause different expansion and contraction behaviours. These

Table 6 Fracture energy of raw and acid-exposure GCFREP hybrid composites

Raw	Fracture Energy (J)		
	-10 °C	25 °C	40 °C
Raw	3.4 (± 0.1)		
Temperature / Duration	-10 °C	25 °C	40 °C
1 day	3.2 (± 0.6) -5.9%↓	2.7 (± 0.7) -20.6%↓	2.5 (± 0.2) -26.5%↓
1 week	3.0 (± 0.6) -11.8%↓	2.4 (± 0.7) -29.4%↓	2.3 (± 0.3) -32.4%↓
3 weeks	3.0 (± 0.6) -11.8%↓	2.1 (± 0.1) -38.2%↓	2.1 (± 0.4) -38.2%↓
6 weeks	3.0 (± 0.3) -11.8%↓	2.4 (± 0.5) -29.4%↓	2.3 (± 0.3) -32.4%↓
9 weeks	3.3 (± 1.0) -2.9%↓	1.9 (± 0.1) -44.1%↓	2.3 (± 0.4) -32.4%↓
12 weeks	3.0 (± 0.4) -11.8%↓	1.9 (± 0.1) -44.1%↓	2.1 (± 0.5) -38.2%↓

differences reveal defects such as microcracking, debonding, and delamination in the interfacial region between fibre and matrix [60]. This may be why the different fracture energy behaviour is stable at low temperatures and tends to decrease at high temperatures.

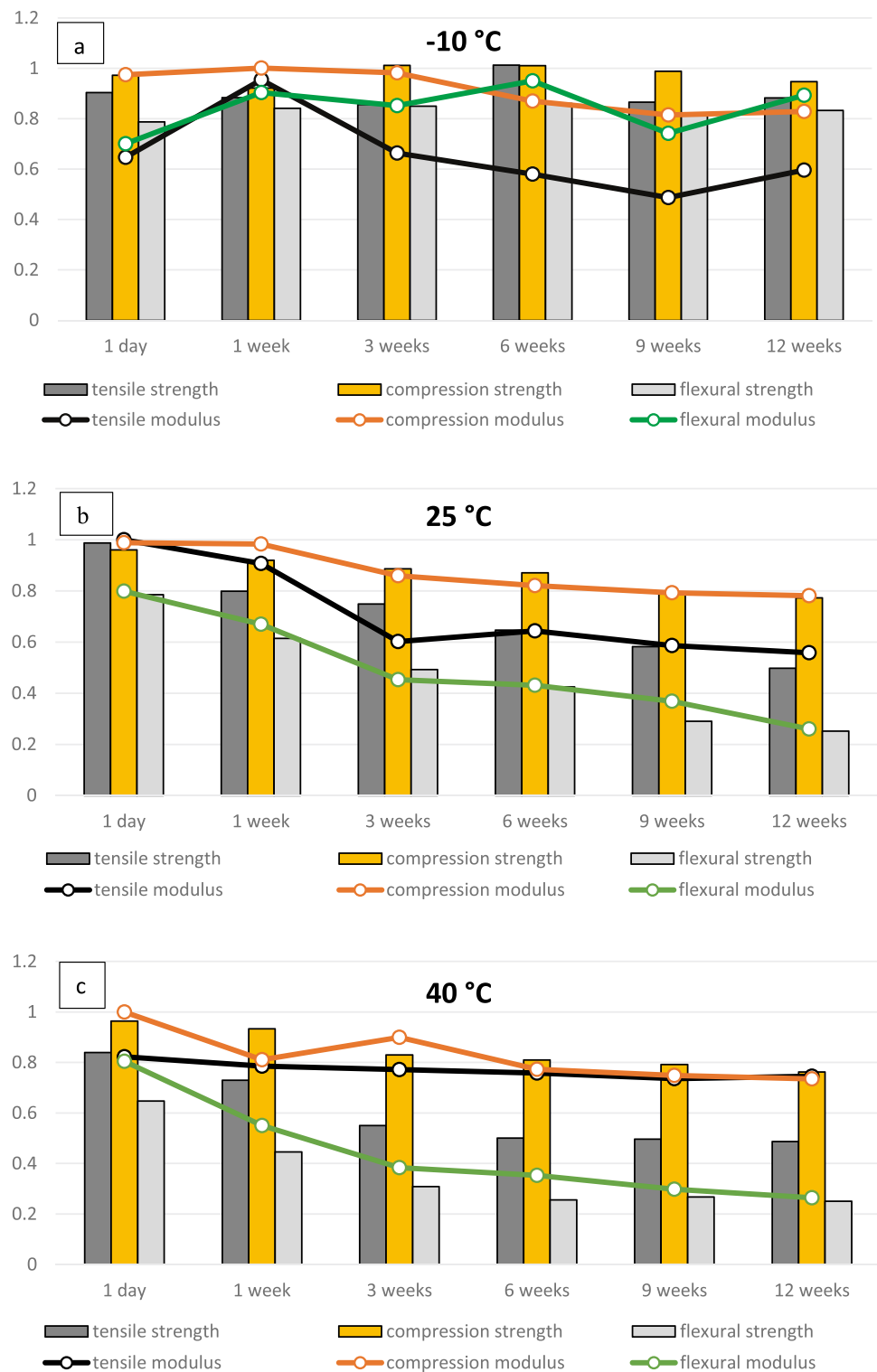
The change in tensile, compressive, and flexural properties of hybrid composites as a function of the duration of acid exposure and the temperature of the acidic environment is shown in Fig. 11. In this graph, all properties are normalised to the properties of the raw specimen. The results show that all properties reduce regardless of the acidic environment temperature. The reduction is more pronounced for flexural loading than other properties. However, flexural strength is more affected by the acidic environment than the flexural modulus. This effect is more significant at 40 °C than at -10 °C. For example, after 12 weeks, flexural strength and flexural modulus have decreased by 16.7% and 10.5%, respectively, compared to the raw material, while at 40 °C, they have decreased by 75.0% and 73.6%, respectively. Reduction in flexural properties is more pronounced than other properties at 40 °C. While both strength and stiffness values are not affected much by exposure to the acidic environment at -10 °C, the sensitivity of specimens at 40 °C to the acidic environment increases. Depending on the exposure time, there is no significant change in the mechanical properties of the samples exposed to the acidic environment at -10 °C. The slight differences that occur when the mechanical test results of these samples are compared can be associated with differences that may arise due to the nature of the production processes.

Comparing the behaviour of the specimens kept at different temperatures in an acidic environment under three different loading conditions shows that the property is least affected under compressive loading. Unlike flexural loading, the effect of the acidic environment on compressive strength is less than the effect on compressive modulus. Considering the behaviour of the hybrid composites under tensile loading, the tensile modulus of the specimens at -10 °C is more affected by the acidic environment, while the tensile strength of specimens at 40 °C is more affected.

Structural properties

FTIR spectra showing the variation of pH 1.0 acid exposure for 12 weeks on the specimens against temperature are given in Fig. 12(a) (FTIR spectra of the specimens at 1, 6, and 12 weeks, along with temperature variations, are given in Fig. S11). The broad band centred at 3380 cm^{-1} corresponds to the O–H stretching of the hydroxyl groups. C–H stretching bands of methyl (CH_2) and methylene (CH_3) groups are observed at 2970 cm^{-1} and 2925 cm^{-1} , respectively. The bands at 1608 cm^{-1} and 1510 cm^{-1} are due to the C = C and

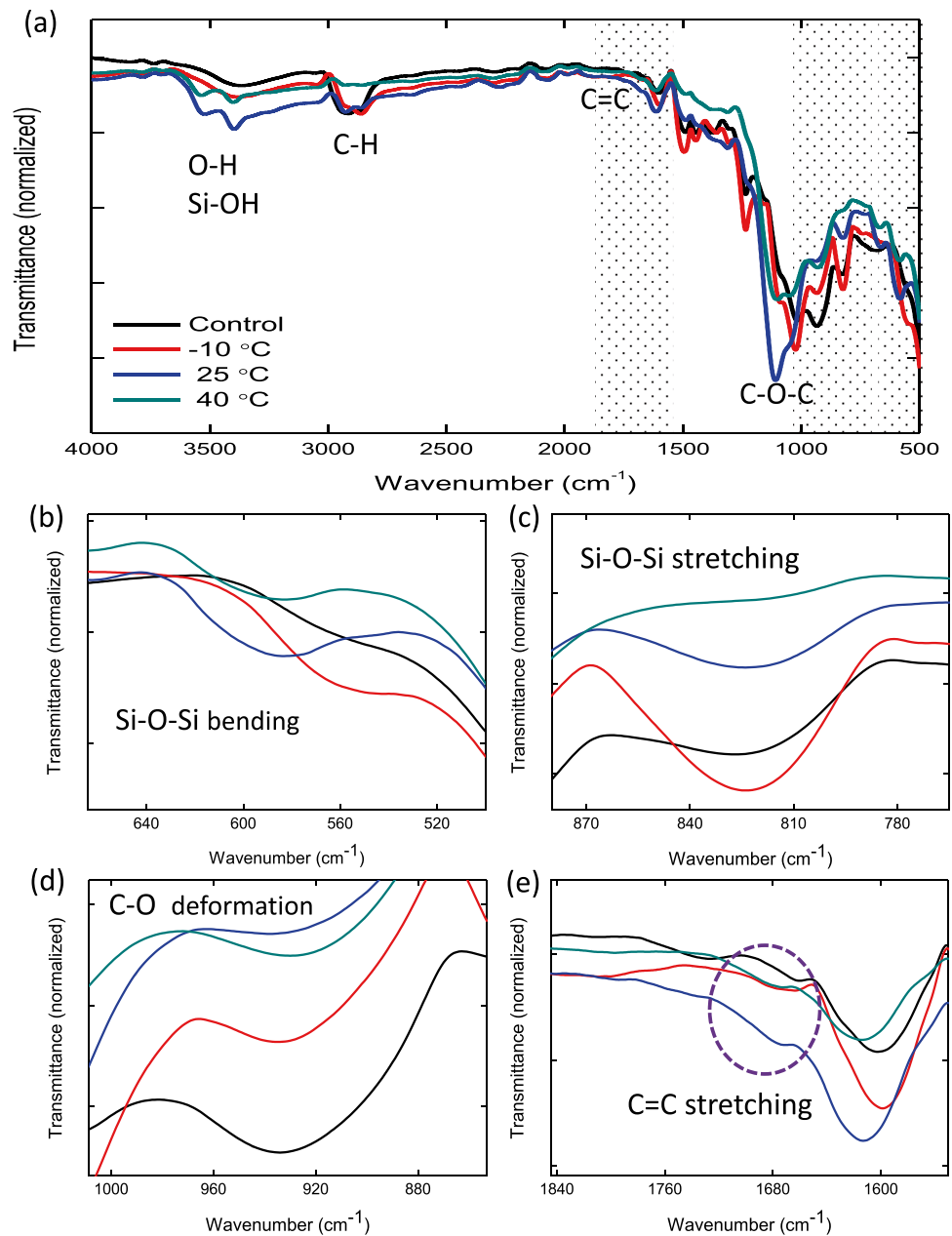
Fig. 11 a Normalized tensile strength-modulus, compressive strength-modulus, and flexural strength-modulus of GCFREP hybrid composites acid-exposed at **a** -10 °C, **b** 25 °C, and **c** 40 °C



C–C stretching vibrations in the aromatic ring of epoxy (diglycidyl ether bisphenol). In addition, C–O bands from C–OH stretching (1180 cm^{-1}) and aryl–alkyl asymmetric stretching (1240 cm^{-1}) are present in all specimens. The specimens underwent a significant chemical change after being treated with an acidic environment at various

temperatures and immersion times. The increase in the intensity of the O–H stretching of the hydroxyl group and the newly formed bands at 3405 and 3540 cm^{-1} indicate the formation of surface Si–OH groups linked by hydrogen bonds to surface water. The hydrolysis of the surface of the glass fibres is likely responsible for the decline in

Fig. 12 **a** FTIR spectra illustrating the impact of pH 1.0 acid exposure on the specimens over 12 weeks at various temperatures, **b-e** Enlarged views of the spectra in the range of 500 and 1000 cm^{-1}



mechanical properties [58]. Si–O–Si stretching (1030 and 824 cm^{-1}) and bending (555 cm^{-1}) vibrations of Si–O (Fig. 12(b-c)) originating from the glass fibres used in the hybrid composites [61]. However, the degradation of glass fibres commenced through dissolution upon exposure to the acidic environment, particularly at 25 °C and 40 °C, as evidenced by the shift in the intensity of Si–O bands compared to those of the control and specimens treated at -10 °C. Furthermore, the C–O deformation of the oxirane ring, which is characteristic of epoxy, is observed at 920 cm^{-1} and decreased with temperature (Fig. 12(d)). This observation suggests the degradation and oxidation of epoxy, which may contribute to

a decline in the mechanical properties because of chain scissions – a result of bond breakage along the polymer chain [62, 63]. Unlike the control specimen another new band formation was observed at 1675 cm^{-1} at all temperatures, and this band may belong to the C = C stretching due to oxidative degradation of epoxy [52].

High temperatures are known to accelerate the degradation processes that result from exposure to acids or alkalis. In the acid-glass fibre interaction, ionic exchange occurs between the metallic cations on the fibre surface and the hydrogen ions in the acid solution [64]. Thus, both thermal and chemical ageing cause deterioration of the mechanical properties (see Figs. 7–9).

Thermal properties

The thermal behaviour of the specimens exposed to acid and different temperatures/immersion times is shown in Fig. 13. The three weight losses observed for the specimens are consecutive to the elimination of absorbed water, the dehydration and decomposition of the epoxy resin, and the conversion of Si–OH to SiO₂. Since the amount of acid solution absorbed in the composites increased with temperature and time, the water loss was the highest in the specimens exposed to acid at 25 °C and 40 °C for 12 weeks compared to other specimens. This finding is consistent with the absorption behaviour of the specimens. The weight of the specimens remains constant at around 550 °C, and the majority of remaining residue originating from glass fibre is anticipated to be composed of SiO₂. From this point of view, since the maximum SiO₂ is observed for the specimen at -10 °C and 12 weeks of acid exposure, glass fibres are preserved at low temperatures,

which is also in line with the FTIR results. The glass fibres start to dissolve, and the remaining SiO₂ amount decreases in comparison to the control specimen after 6 weeks at 25 °C. As the temperature is further raised, the glass fibres begin to dissolve as early as the first week, and the amount of SiO₂ continues to decline as exposure time increases. In summary, it has been found that the thermal stability value is decreased by longer exposure times for specimens kept in an acidic environment. The specimens treated at 40 °C were shown to be the most adversely affected.

Thermograms were obtained with DSC analyses to observe the effects of acidic environments at various exposure temperatures and durations on the glass transition temperatures (T_g) of GCFREP hybrid composite materials. In the DSC thermogram, the upper transition peaks indicate the heat requiring an endothermic zone, while the lower transition peaks indicate the heat melting exothermic zone. Decomposition temperatures are obtained from endothermic transition peaks. T_g represents the temperature region

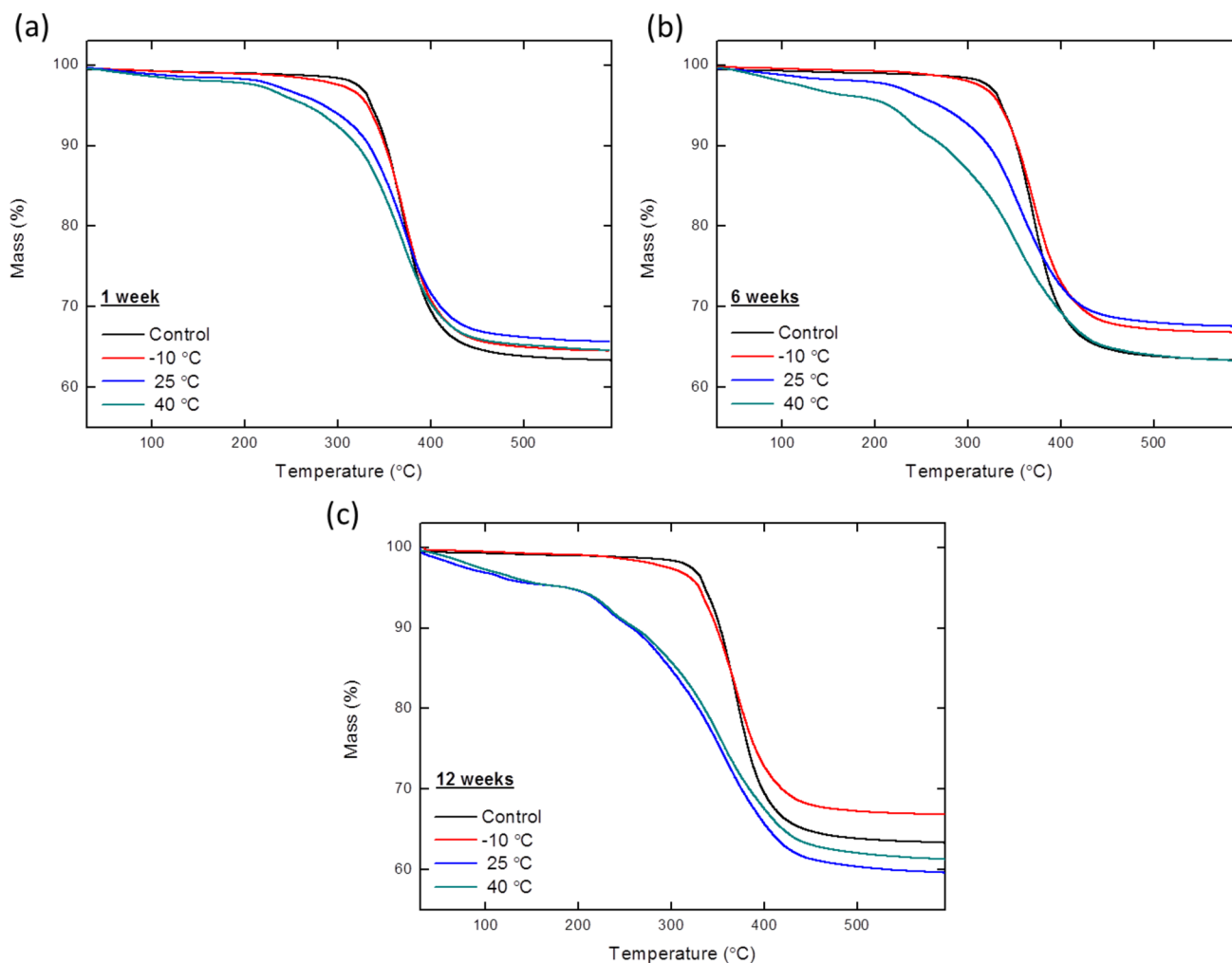


Fig. 13 TGA curves showing the variation of pH 1.0 acid exposure on the specimens versus temperature and time

where the polymer changes from a rigid, glassy structure to a rubbery structure. T_g characterises the amorphous region feature of the polymers.

T_g can be affected by ageing, thermal/chemical applications, polymer chemistry, and degree of crystallinity. Chemical environment exposure may cause some changes in the polymer molecular chain structure. Figure 14 presents DSC thermograms of the specimens in the pH 1.0 acidic environment at 10, 25, and 40 °C for 1, 6, and 12 weeks. In addition, the glass transition temperatures (T_g) calculated from the thermograms are listed in Table 7. The changes in characteristic temperatures given in the table directly affect design considerations. In particular, the value of T_g is an important parameter to consider in determining the maximum service temperature of polymeric composites. Operating the composites at temperatures above the T_g value causes them to be unable to maintain their solid state and decreases their mechanical strength. Accordingly, compared to the raw specimens, it can be seen that the T_g increases relatively

Table 7 Glass transition temperatures of specimens exposed to pH 1.0 acidic environment

Raw	T_g (°C)		
	-10 °C	25 °C	40 °C
Raw	65.9		
Temperature / Duration	-10 °C	25 °C	40 °C
1 week	66.3 0.6%↑	65.0 -1.4%↓	66.6 1.1%↑
6 weeks	64.1 -2.7%↓	69.2 5.0%↑	71.1 7.9%↑
12 weeks	65.5 -0.6%↓	81.6 23.8%↑	78.2 18.7%↑

for all specimens. This is inconsistent with results where there is a loss in specimen stiffness and an increase in failure strain. The T_g of the raw specimens is found to be 65.88 °C. In specimens exposed to the acidic environment at 25 and

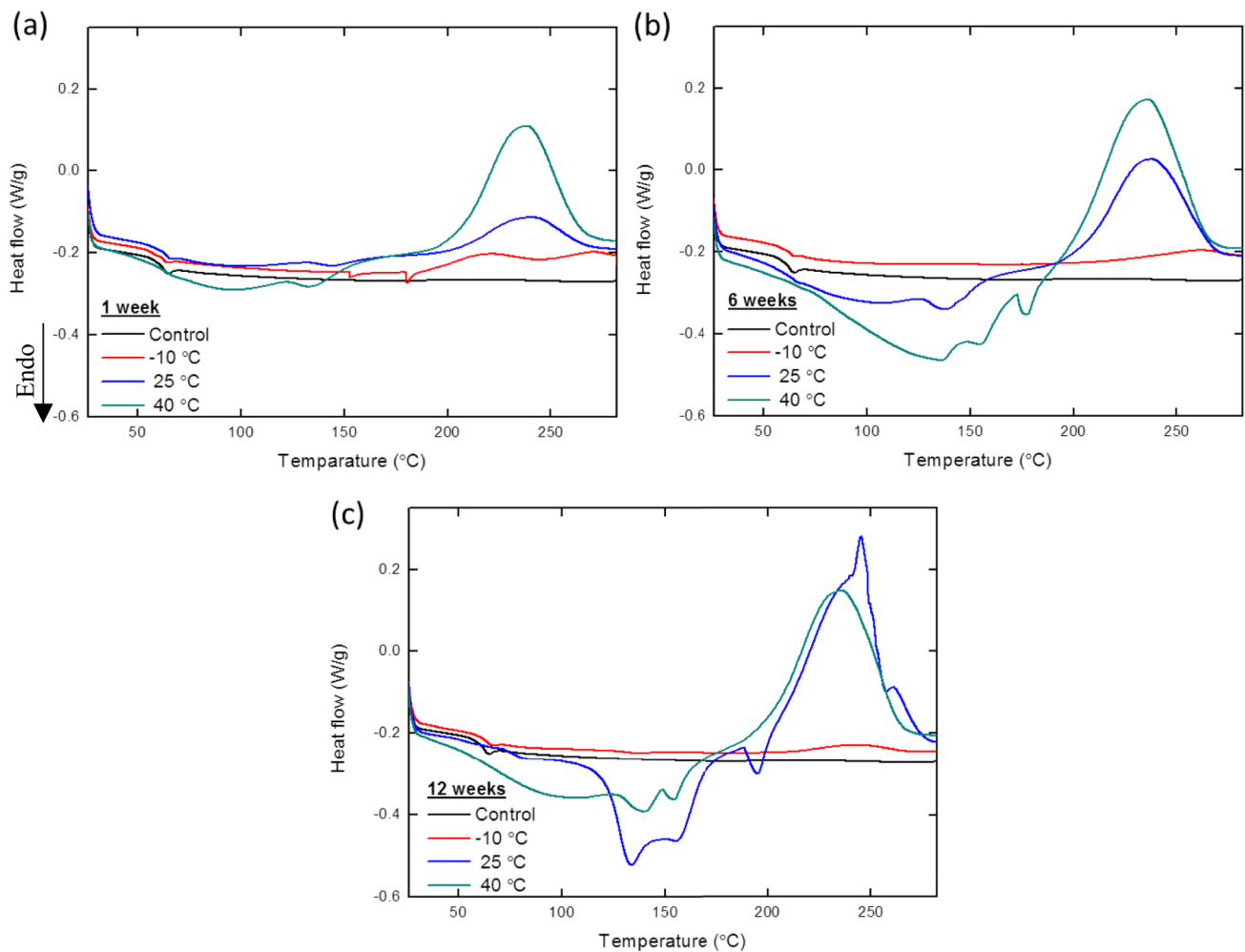


Fig. 14 DSC thermogram showing the variation of pH 1.0 acid exposure on the specimens versus temperature and time

40 °C, the T_g increases with increasing exposure time, while the T_g at -10 °C is almost unchanged and exhibits properties similar to those of the raw specimens. This increase in T_g is attributed to the steric hindrance effect provided by benzene rings in the epoxy resin and an increase in crosslinking density, which reduces the mobility of the polymer chains [65]. Upon acid exposure, penetration of ions through the aqueous systems into the composites can limit the segmental interactions, thereby enhancing T_g [66]. Similar results have been reported in our previous work [67, 68].

Conclusion

This study investigated the effects of concentrated sulfuric acid (H_2SO_4) and nitric acid (HNO_3) based simulated acidic rain solvent on absorptive, morphological, mechanical, structural, and thermal properties of GCFREP hybrid composites. The selected durations for exposure to the pH 1.0 acidic environment were 1 day, 1 week, 3, 6, 9, and 12 weeks, and ambient temperatures were -10, 25, and 40 °C. After the specimens were exposed to the acidic environment under the specified conditions, they were subjected to characterisation tests. Accordingly, the following findings were itemised.

- Due to the degradation reaction that occurs due to long-term physical and chemical ageing, changes occur in both the mechanical and thermal properties of hybrid composites. A strong correlation is observed between acid diffusion and mechanical/thermal properties.
- Based on the absorption tests, the immersion duration for specimens to partially saturate with the acidic solvent is estimated to be approximately 6 weeks for those exposed at 40 °C and 9 weeks for those exposed at 25 °C. Maximum weight gain is observed after 12 weeks of exposure in all specimens. After 12 weeks of immersion, maximum weight gains of approximately 7.9%, 7%, and 0.6% are obtained for specimens exposed at 40, 25, and -10 °C, respectively.
- Regarding aesthetics, after 12 weeks of exposure to a pH 1.0 acidic environment, a slight discolouration is observed in the specimens exposed at -10 °C, while the most noticeable colour change is observed in those exposed at 40 °C.
- It has been revealed that the temperature of the acidic environment and its exposure time affect all mechanical properties. When evaluating the strength of GCFREP hybrid composites, the maximum tensile, compression, and flexural strength reduction is 51.4%, 23.9%, and 75.0%, respectively, in the specimens exposed to pH 1.0 acidic environment at 40 °C for 12 weeks.
- Experimental results have shown that tensile moduli of the specimens kept at pH 1.0 at -10 °C tend to decrease after 1 week, and compression moduli decrease after 3 weeks. The tensile, compressive, and flexural modulus of the specimens kept at pH 1.0 at 25 °C decrease with prolonged exposure times. While the tensile and compression moduli of the specimens kept at pH 1.0 at 40 °C do not change, the flexural moduli show a continuous downward trend.
- When absorption test data and mechanical properties are considered together, diffusion can accelerate the reduction of mechanical properties, and the presence of this reduction or damage may accelerate the penetration of acidic solutions.
- The absorption and TGA analyses are consistent with the amount of acidic solution absorbed and lost. The highest amount of moisture absorbed and lost is seen in samples exposed for 12 weeks at 25 and 40 °C.
- When the thermal stability values of GCFREP hybrid composites are examined, it is revealed that the most critical decrease occurs in the specimens exposed at 40 °C for 12 weeks to the pH 1.0 acidic environment, and it has been found that prolonged exposure durations have an inversely proportional effect on thermal stability values.

Supplementary Information The online version contains supplementary material available at <https://doi.org/10.1007/s10965-023-03860-x>.

Acknowledgements The authors would like to acknowledge the support of The Scientific and Technological Research Council of Türkiye (TÜBİTAK) under Grant no. 120M158. All authors are truly grateful for the support.

Funding The Scientific and Technological Research Council of Türkiye (TÜBİTAK), 120M158, Buket Okutan Baba

Declarations

Conflict of interest The authors declare that they have no known competing financial interests or personal relationships that could have appeared to influence the work reported in this paper.

References

1. Gibson RF (2016) Principles of composite material mechanics. Boca Raton, Florida, United States
2. Reddy JN (2003) Mechanics of laminated composite plates and shells. Boca Raton, Florida, United States
3. Kaw AK (2005) Mechanics of composite materials, 2nd edn. CRC Press
4. Nurazzi NM, Asyraf MRM, Fatimah Athiyah S et al (2021) A review on mechanical performance of hybrid natural fiber polymer composites for structural applications. *Polymers (Basel)* 13(13):2170

5. Nguyen H, Zatar W, Mutsuyoshi H (2017) Hybrid polymer composites for structural applications. Hybrid polymer composite materials: applications. Woodhead Publications, Cambridge, UK
6. Swolfs Y, Gorbatiikh L, Verpoest I (2014) Fibre hybridisation in polymer composites: A review. *Compos Part A Appl Sci Manuf* 67:181–200
7. Hayashi T (1972) On the improvement of mechanical properties of composites by hybrid composition. 8th international reinforced plastics conference. British Plastic Federation, Brighton
8. Bunsell AR, Harris B (1974) Hybrid carbon and glass fibre composites. *Composites* 5:157–164. [https://doi.org/10.1016/0010-4361\(74\)90107-4](https://doi.org/10.1016/0010-4361(74)90107-4)
9. Manders PW, Bader MG (1981) The strength of hybrid glass/carbon fibre composites - Part 1 Failure strain enhancement and failure mode. *J Mater Sci* 16:2233–2245. <https://doi.org/10.1007/BF00542386>
10. Pimenta S, Pinho ST (2013) Hierarchical scaling law for the strength of composite fibre bundles. *J Mech Phys Solids* 61:1337–1356. <https://doi.org/10.1016/j.jmps.2013.02.004>
11. Swolfs Y, Gorbatiikh L, Verpoest I (2013) Stress concentrations in hybrid unidirectional fibre-reinforced composites with random fibre packings. *Compos Sci Technol* 85:10–16. <https://doi.org/10.1016/j.compscitech.2013.05.013>
12. Swolfs Y, Gorbatiikh L, Romanov V et al (2013) Stress concentrations in an impregnated fibre bundle with random fibre packing. *Compos Sci Technol* 74:113–120. <https://doi.org/10.1016/j.compscitech.2012.10.013>
13. Xing J, Hsiao GC, Chou TW (1981) A dynamic explanation of the hybrid effect. *J Compos Mater* 15:443–461. <https://doi.org/10.1177/002199838101500504>
14. Ravishankar B, Nayak SK, Kader MA (2019) Hybrid composites for automotive applications – A review. *J Reinf Plast Compos* 38:835–845. <https://doi.org/10.1177/0731684419849708>
15. Chauhan A, Kumar M, Kumar S (2021) Fabrication of polymer hybrid composites for automobile leaf spring application. *Mater Today Proc* 48(5):1371–1377
16. Kolpachkov ED, Kurnosov AO, Petrova AP, Raskutin AE (2020) Fiber-based hybrid polymer composites for aviation: a review. *Vopr Materialoved* 1:126–138. <https://doi.org/10.22349/1994-6716-2020-101-1-126-138>
17. Raj K, Vasudevan A, Pugazhendhi L (2021) A review on different hybrid composites for aircraft structures. *Mater Today Proc*. <https://doi.org/10.1016/j.matpr.2020.10.774>
18. Gururaja MN, Rao ANH (2012) A review on recent applications and future prospectus of hybrid composites. *Int J Soft Comput Eng* 1(6):352–355
19. Jagadeesh P, Puttegowda M, Girijappa YGT et al (2022) Carbon fiber reinforced areca/sisal hybrid composites for railway interior applications: mechanical and morphological properties. *Polym Compos* 43:160–172. <https://doi.org/10.1002/pc.26364>
20. Dinesh S, Elanchezhian C, Vijayarajam B et al (2020) Experimental investigation of natural and synthetic hybrid composite for marine application. *Mater Today Proc* 22(3):322–329
21. Fiore V, Di Bella G, Valenza A (2011) Glass-basalt/epoxy hybrid composites for marine applications. *Mater Des* 32:2091–2099. <https://doi.org/10.1016/j.matdes.2010.11.043>
22. Swolfs Y (2017) Perspective for fibre-hybrid composites in wind energy applications. *Materials (Basel)* 10(11):1–17
23. Reddy SSP, Suresh R, Hanamantraygouda MB, Shivakumar BP (2021) Use of composite materials and hybrid composites in wind turbine blades. *Mater Today Proc* 46(7):2827–2830
24. Zhang J, Chaisombat K, He S, Wang CH (2012) Glass/carbon fibre hybrid composite laminates for structural applications in automotive vehicles. *Sustainable automotive technologies*. Springer, Berlin, Heidelberg
25. Bhagwat PM, Ramachandran M, Raichurkar P (2017) Mechanical properties of hybrid glass/carbon fiber reinforced epoxy composites. *Mater Today Proc* 4:7375–7380
26. Jesthi DK, Nayak RK (2019) Improvement of mechanical properties of hybrid composites through interply rearrangement of glass and carbon woven fabrics for marine application. *Compos Part B Eng* 168:467–475. <https://doi.org/10.1016/j.compositesb.2019.03.042>
27. Summerscales J (2019) *Materials selection for marine composites*. Marine composites. Elsevier Ltd, Amsterdam, Holland
28. Wahrhaftig A, Ribeiro H, Nogueira A (2019) A structural composite for marine boat constructions. *Marine composites*. Woodhead Publishing, Cambridge, UK
29. Metyx composites (2017) The world's largest carbon hybrid composite catamaran. https://www.metyx.com/wp-content/uploads/PDF_Files/Marin_Brochure.pdf. Accessed 15 Jan 2024
30. Summerscales J, Short D (1978) Carbon fibre and glass fibre hybrid reinforced plastics. *Composites* 9:157–166. [https://doi.org/10.1016/0010-4361\(78\)90341-5](https://doi.org/10.1016/0010-4361(78)90341-5)
31. Chandra DS, Reddy KVK, Hebbal O (2018) Fabrication and mechanical characterisation of glass and carbon fibre reinforced composite's used for marine applications. *Int J Eng Technol* 7:228–232. <https://doi.org/10.14419/ijet.v7i4.5.20052>
32. Mishnaevsky L, Branner K, Petersen HN et al (2017) Materials for wind turbine blades: an overview. *Materials (Basel)* 10(11):1–24
33. Mishnaevsky L, Dai G (2014) Hybrid carbon/glass fiber composites: micromechanical analysis of structure-damage resistance relationships. *Comput Mater Sci* 81:630–640. <https://doi.org/10.1016/j.commatsci.2013.08.024>
34. Raji M, Zari N, Bouhfid R, El Kacem Qaiss A (2018) Durability of composite materials during hydrothermal and environmental aging. Durability and life prediction in biocomposites, fibre-reinforced composites and hybrid composites. Woodhead Publishing, Cambridge, UK
35. Burns DA, Aherne J, Gay DA, Lehmann CMB (2016) Acid rain and its environmental effects: Recent scientific advances. *Atmos Environ* 146:1–4
36. Sanliyüksel Yücel D, Balci N, Baba A (2016) Generation of acid mine lakes associated with abandoned coal mines in Northwest Turkey. *Arch Environ Contam Toxicol* 70:757. <https://doi.org/10.1007/s00244-016-0270-z>
37. Löhr AJ, Bogaard TA, Heikens A et al (2005) Natural pollution caused by the extremely acidic crater lake Kawah Ijen, East Java. *Indonesia Environ Sci Pollut Res* 12:89–95
38. Qiu Q, Kumosa M (1997) Corrosion of E-glass fibers in acidic environments. *Compos Sci Technol* 57:497–507. [https://doi.org/10.1016/S0266-3538\(96\)00158-3](https://doi.org/10.1016/S0266-3538(96)00158-3)
39. Xue Y, Veazie DR, Glinsey C et al (2007) Environmental effects on the mechanical and thermomechanical properties of aspen fiber-polypropylene composites. *Compos Part B Eng* 38:152–158. <https://doi.org/10.1016/j.compositesb.2006.07.005>
40. Buck SE, Lischer DW, Nemat-Nasser S (2001) Mechanical and microstructural properties of notched E-glass/vinyl ester composite materials subjected to the environment and a sustained load. *Mater Sci Eng A* 317:128–134. [https://doi.org/10.1016/S0921-5093\(01\)01170-4](https://doi.org/10.1016/S0921-5093(01)01170-4)
41. John K, Naidu SV (2007) Chemical resistance of sisal/glass reinforced unsaturated polyester hybrid composites. *J Reinf Plast Compos* 26:373–376. <https://doi.org/10.1177/0731684406072524>
42. Singh P, Kaushik A, Kaur K (2005) Mechanical properties and swelling behavior of short glass fiber reinforced polyester composites. *J Thermoplast Compos Mater* 18:543–559. <https://doi.org/10.1177/0892705705055444>
43. Amaro AM, Reis PNB, Neto MA, Louro C (2013) Effects of alkaline and acid solutions on glass/epoxy composites. *Polym Degrad*

- Stab 98:853–862. <https://doi.org/10.1016/j.polymdegradstab.2012.12.029>
44. Pai R, Kamath MS, Rao RMVGK (1997) Acid resistance of glass fibre composites with different lay-up sequencing part II: degradation studies. *J Reinf Plast Compos* 16:1013–1019. <https://doi.org/10.1177/073168449701601103>
 45. Pai R, Kamath MS, Rao RMVGK (1997) Acid resistance of glass fibre composites with different lay-up sequencing: Part I-diffusion studies. *J Reinf Plast Compos* 16:1002–1012. <https://doi.org/10.1177/073168449701601102>
 46. Mahmoud MK, Tantawi SH (2003) Effect of strong acids on mechanical properties of glass/polyester GRP pipe at normal and high temperatures. *Polym Plast Technol Eng* 42:677–688. <https://doi.org/10.1081/PPT-120023102>
 47. Huntsman (2020) Advanced materials. https://www.huntsman.com/docs/Documents/20p_Resin_144699_Huntsman_Composites.pdf. Accessed 15 Jan 2024
 48. Li Y, Wang Y, Wang Y, Wang B (2019) Effects of simulated acid rain on soil respiration and its component in a mixed coniferous-broadleaved forest of the three gorges reservoir area in Southwest China. *For Ecosyst* 6:32. <https://doi.org/10.1186/s40663-019-0192-0>
 49. Weitsman YJ (2000) Effects of fluids on polymeric composites—a review. *Compr Compos Mater* 2:369–401
 50. Barjasteh E, Nutt SR (2012) Moisture absorption of unidirectional hybrid composites. *Compos Part A Appl Sci Manuf* 43:158–164. <https://doi.org/10.1016/j.compositesa.2011.10.003>
 51. Martin R (2008) Ageing of composites. Woodhead Publishing, Cambridge, UK
 52. Chauhan A, Bedi HS, Agnihotri PK (2022) Enhancing aging resistance of glass fiber/epoxy composites using carbon nanotubes. *Mater Chem Phys* 291:126740. <https://doi.org/10.1016/j.matchemphys.2022.126740>
 53. Osei Bonsu A, Liang W, Mensah C, Yang B (2022) Assessing the mechanical behavior of glass and basalt reinforced vinyl ester composite under artificial seawater environment. *Structures* 38:961–978. <https://doi.org/10.1016/j.istruc.2022.02.053>
 54. Li H, Zhang K, Fan X et al (2019) Effect of seawater ageing with different temperatures and concentrations on static/dynamic mechanical properties of carbon fiber reinforced polymer composites. *Compos Part B Eng* 173:106910. <https://doi.org/10.1016/j.compositesb.2019.106910>
 55. Schultheisz CR, Waas AM (1996) Compressive failure of composites, Part I: Testing and micromechanical theories. *Prog Aerosp Sci* 32(1):1–42
 56. Opelt CV, Cândido GM, Rezende MC (2018) Compressive failure of fiber reinforced polymer composites – A fractographic study of the compression failure modes. *Mater Today Commun* 15:218–227. <https://doi.org/10.1016/j.mtcomm.2018.03.012>
 57. Budiansky B, Fleck NA (1993) Compressive failure of fibre composites. *J Mech Phys Solids* 41:183–211. [https://doi.org/10.1016/0022-5096\(93\)90068-Q](https://doi.org/10.1016/0022-5096(93)90068-Q)
 58. Bonsu AO, Mensah C, Liang W et al (2022) Mechanical degradation and failure analysis of different glass/basalt hybrid composite configuration in simulated marine condition. *Polymers (Basel)* 14:3480. <https://doi.org/10.3390/polym14173480>
 59. Dong C, Ranaweera-Jayawardena HA, Davies IJ (2012) Flexural properties of hybrid composites reinforced by S-2 glass and T700S carbon fibres. *Compos Part B Eng* 43:573–581. <https://doi.org/10.1016/j.compositesb.2011.09.001>
 60. Hulugappa B, Achutha MV, Suresha B (2016) Effect of environmental conditions on flexural strength and fracture toughness of particulate filled glass-epoxy hybrid composites. *Mater Sci Appl* 7:710–729. <https://doi.org/10.4236/msa.2016.711057>
 61. Bonon AJ, Weck M, Bonfante EA, Coelho PG (2016) Physico-chemical characterisation of three fiber-reinforced epoxide-based composites for dental applications. *Mater Sci Eng C* 69:905–913. <https://doi.org/10.1016/j.msec.2016.07.002>
 62. González MG, Cabanelas JC, Baselga J (2012) Applications of FTIR on epoxy resins - identification, monitoring the curing process, phase separation and water uptake. *Infrared spectroscopy - materials science, engineering and technology*. IntechOpen Ltd., London, UK
 63. Örtengren U, Wellendorf H, Karlsson S, Ruyter IE (2001) Water sorption and solubility of dental composites and identification of monomers released in an aqueous environment. *J Oral Rehabil* 28:1106–1115. <https://doi.org/10.1046/j.1365-2842.2001.00802.x>
 64. Maxwell A. S, Broughton WR, Dean G, Sims GD, (2005) Review of accelerated ageing methods and lifetime prediction technique for polymeric materials. Crown, Middlesex, UK
 65. Amini M, Khavandi A (2019) Synergistic effects of mechanical and environmental loading in stress corrosion cracking of glass/polymer composites. *J Compos Mater* 53:3433–3444. <https://doi.org/10.1177/0021998319842376>
 66. Uthaman A, Xian G, Thomas S et al (2020) Durability of an epoxy resin and its carbon fiber-reinforced polymer composite upon immersion in water, acidic, and alkaline solutions. *Polymers (Basel)* 12:614. <https://doi.org/10.3390/polym12030614>
 67. Akderya T, Özmen U, Baba BO (2020) Investigation of long-term ageing effect on the thermal properties of chicken feather fibre/poly(lactic acid) biocomposites. *J Polym Res* 27:162. <https://doi.org/10.1007/s10965-020-02132-2>
 68. Akderya T, Özmen U, Baba BO (2021) Revealing the long-term ageing effect on the mechanical properties of chicken feather fibre/poly(lactic acid) biocomposites. *Fibers Polym* 22:2602–2611. <https://doi.org/10.1007/s12221-021-0304-7>

Publisher's Note Springer Nature remains neutral with regard to jurisdictional claims in published maps and institutional affiliations.

Springer Nature or its licensor (e.g. a society or other partner) holds exclusive rights to this article under a publishing agreement with the author(s) or other rightsholder(s); author self-archiving of the accepted manuscript version of this article is solely governed by the terms of such publishing agreement and applicable law.